DOI: 10.1002/chem.200600986

Synthesis and Characteristics of a Nonaggregating Tris(tetrathiafulvaleno)dodecadehydro[18]annulene

Asbjørn Sune Andersson,[a, b] Kristine Kilså,[b, c] Tue Hassenkam,[c] Jean-Paul Gisselbrecht,[d] Corinne Boudon,[d] Maurice Gross,[d] Mogens Brøndsted Nielsen,*[b] and François Diederich*[a]

Abstract: A new tris(tetrathiafulvaleno)dodecadehydro[18]annulene with six peripheral *n*-hexyl substituents was prepared by oxidative Glaser–Hay cyclization of a corresponding diethynylated tetrathiafulvalene (TTF) precursor. The electronic properties of the neutral and oxidized species were studied by both UV/Vis absorption spectroscopy and electrochemistry. From these studies, it transpires that the strongly violet-colored macrocycle does not aggregate in solution to any significant degree, which was confirmed by ^{1}H NMR spectroscopy. This reluctance towards aggregation contrasts that observed for related TTF–annulenes containing other peripheral substitutents. Oxidation of the TTF–annulene occurs in two three-electron steps as inferred from both the peak amplitudes and the spectroelectrochemical study. We find that the tris(TTF)-fused dehydro[18]annulene is more difficult to oxidize (by +0.20 V) than the silyl-protected diethynylated mono-TTF precursor. In contrast, the first vertical ionization energy calculated at the B3LYP/6–311+G(2d,p) level for the parent tris(TTF)-fused dehydro[18]annulene devoid of peripheral hexyl substituents is in fact lower (by 0.44 eV). Moreover, the surface morphology of **1d** drop-cast on a mica substrate was investigated by atomic force microscopy (AFM). Crystalline domains with slightly different orientations were observed. The thickness of individual layers seen in the crystalline domains and the thickness of a monolayer obtained from a very dilute solution were determined to 1.8–1.9 nm. This thickness corresponds to the diameter of the macrocycle and the layers seen in the film are apparently formed when the molecules stack in the horizontal direction relative to the substrate.

Keywords: aggregation · alkynes · cyclization · dehydroannulenes · tetrathiafulvalenes

Introduction

For more than three decades, tetrathiafulvalene (TTF) and its derivatives have been studied on account of their unique π-electron-donor properties.[1] Effective methods have been developed for the preparation of elaborate molecular architectures containing TTF moieties,

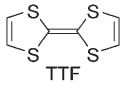

TTF

such as macrocycles, cyclophanes, cages, catenanes, rotaxanes, dendrimers, and polymers, which are of interest for both materials and supramolecular chemistry.[1] Acetylenic scaffolding[2] with ethynylated derivatives of TTF[3–5] as well as of its dithiafulvene "half-unit"[6] presents one such method for constructing highly conjugated optoelectronic materials.

Rubin and co-workers[4] suggested in 1998 the tris(tetrathiafulvaleno)dodecadehydro[18]annulene macrocycle **1a** as an interesting target molecule with potential to form con-

[a] A. S. Andersson, Prof. Dr. F. Diederich
Laboratorium für Organische Chemie, ETH Zürich, HCI
8093 Zürich (Switzerland)
Fax: (+41) 44-632-1109
E-mail: diederich@org.chem.ethz.ch

[b] A. S. Andersson, Prof. Dr. K. Kilså, Prof. Dr. M. Brøndsted Nielsen
Department of Chemistry, University of Copenhagen
Universitetsparken 5, 2100 Copenhagen Ø (Denmark)
Fax: (+45) 3532-0212
E-mail: mbn@kiku.dk

[c] Prof. Dr. K. Kilså, Prof. Dr. T. Hassenkam
Nano-Science Center, University of Copenhagen
Universitetsparken 5, 2100 Copenhagen Ø (Denmark)

[d] Dr. J.-P. Gisselbrecht, Prof. Dr. C. Boudon, Prof. Dr. M. Gross
Laboratoire d'Electrochimie et de Chimie Physique du Corps Solide
UMR 7177, C.N.R.S, Université Louis Pasteur
4, rue Blaise Pascal, 67000 Strasbourg (France)

Supporting information for this article is available on the WWW under http://www.chemeurj.org/ or from the author.

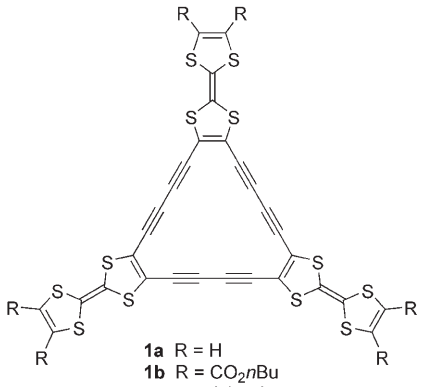

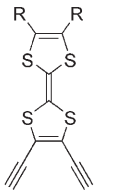

ductive charge-transfer salts. Yet only recently, after completion of the present study, Iyoda and co-workers[5] reported the synthesis of the first derivatives **1b** and **1c**, containing electron-withdrawing ester groups as peripheral substituents. These macrocycles were prepared from the monomeric precursors **2b** and **2c**, respectively, and showed a remarkable propensity for π–π stacking aggregation in apolar aromatic solvents.

In parallel to that work, we had targeted macrocycle **1d** containing six peripheral *n*-hexyl groups to ensure solubility in organic solvents. These groups were expected to slightly increase the electron-donating properties of the TTF moieties, resulting in more efficient intramolecular charge-transfer interactions of these entities with the electron-accepting all-carbon core.[7] Here, we describe the synthesis of tris(TTF)-fused dehydro[18]annulene **1d** and report its optical and electrochemical properties which differ strongly from those of **1b** and **1c** with peripheral electron-accepting ester substituents. In sharp contrast to the last two macrocycles, hexyl-substituted **1d** is reluctant to aggregate in apolar aromatic solvents; this result demonstrates the important contributions of the ester groups in **1b** and **1c** to self-association. These groups greatly extend the π-conjugated perimeter, and interactions between the local ester dipoles may additionally assist aggregation.[8,9] Furthermore, it is well established by the work of Hunter and Sanders[10] that electron-withdrawing substituents favor aromatic π–π stacking interactions by changing the electrostatic properties of the chromophores.[8]

Results and Discussion

Synthesis: The synthesis of macrocycle **1d** was accomplished by using the route outlined in Scheme 1. After consulting the literature about the preparation of nonsymmetrically substituted TTFs,[11] we decided to prepare the 4,5-diethynylated, 4′,5′-dihexyl-substituted **2d** by a Horner–Wadsworth–Emmons condensation, which avoids formation of unwanted symmetrically substituted TTF.

The readily available acyloin **3**[12] was treated with PPh_3 and CCl_4 to give the corresponding α-chloroketone **4** in nearly quantitative yield, which in turn was converted to compound **5** by reaction with potassium piperidine-1-carbodithioate[13] in acetone. Concentrated sulfuric acid affected ring closing and dehydration, and the crude hexafluorophosphate salt **6** was isolated in good yield.[14] Next, the known phosphonate ester **7**[15] was deprotonated with *n*BuLi at −78 °C, which was followed by addition of electrophile **6**. Subsequent treatment with acetic acid at room temperature gave 4,5-dihexyl-substituted TTF **8** in 73% yield. Deprotonation of **8** using an excess of lithium diisopropylamide (LDA) in THF at −78 °C gave the dilithiated TTF, which was trapped with 1,2-diiodoethane to afford **9** in high yield. The subsequent conversion to **10** was achieved by using a Sonogashira cross-coupling reaction[16] with triisopropylsilylacetylene. This conversion was accompanied by the formation of mono-coupled hydrodeiodinated TTF as a byproduct, which caused trouble for the column chromatographic purification on account of the small polarity differences between mono-alkynylated byproduct and dialkynylated **10**. The hydrodehalogenation side reaction in the Sonogashira cross-coupling has been reported by others[17] and seems to be more pronounced for electrophiles containing more than one halogen atom. Desilylation of **10** was accomplished with Bu_4NF in wet THF, and the resulting unstable terminal diyne **2d** was not isolated, but immediately subjected to an oxidative Hay-coupling protocol[18] to give the strongly violet-colored annulene **1d** in 47% yield.

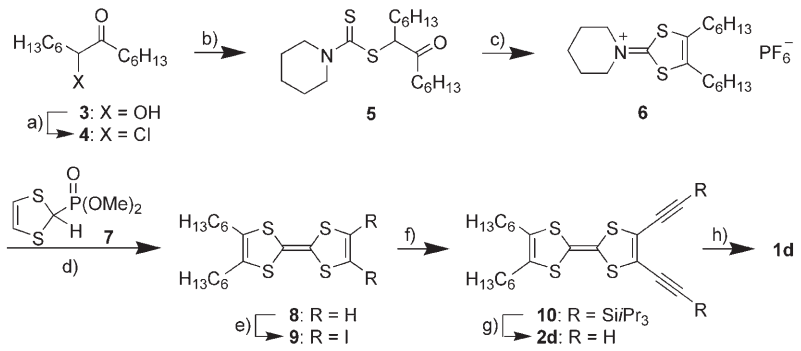

Scheme 1. Synthesis of tris(tetrathiafulvaleno)dodecahydro[18]annulene **1d**. a) CCl_4, PPh_3, MeCN, 97%; b) potassium piperidine-1-carbodithioate, acetone, 88%; c) conc. H_2SO_4, 0 °C, then HPF_6 (aq) 0 °C, 85%; d) *n*BuLi, THF, −78 °C, **7**, then −78 °C→25 °C, AcOH, 73%; e) LDA, THF, −78 °C, then ICH_2CH_2I, 88%; f) $iPr_3SiC{\equiv}CH$, CuI, $[PdCl_2(PPh_3)_2]$, Et_3N, 69%; g) nBu_4NF, THF, 0 °C; h) CuCl, TMEDA, O_2, CH_2Cl_2, 0 °C, 47% (steps g and h). LDA = lithium diisopropylamide; TMEDA = *N*,*N*,*N*′,*N*′-tetramethylethylenediamine.

In contrast to the findings for oxidative coupling of *cis*-bisdeprotected tetraethynylethenes,[7,19] the formation of cyclic dimers was not observed in the Hay coupling of **2d**. From X-ray crystallographic analysis, the inner C(sp)–C≡C bond angles in the strained tetraalkynylatead octadehydro[12]annulene were determined to 117.6° and 118.5°.[19] Calculations on **1a** and **2a** (vide infra) revealed instead C(sp)–C≡C bond angles of 124.8° and 123.9°, respectively. Thus, formation of the cyclic trimer **1d** from **2d** only requires a minor decrease in this bond angle. It seems reasonable to assume that the much larger bond angle deviation required for formation of the cyclic dimer is thwarted by annulation of the five-membered ring in the latter and therefore the pathway leading to the octadehydro[12]annulene cannot compete with the formation of the trimer.

Differential scanning calorimetry (DSC) of **1d** in the temperature range from 25 to 250 °C showed an exothermic drop starting at ca. 100 °C (see Supporting Information). As this process was irreversible, it must correspond to a decomposition reaction. Thus, no endothermic melting process was observed upon further heating. The decomposed material was completely insoluble in organic solvents.

^{1}H NMR spectroscopy: To investigate the degree of aggregation of **1d**, we performed ^{1}H NMR spectroscopic studies in C_6D_6. The resonances for the TTF-CH_2 protons only change very slightly from $\delta = 2.112$ ppm to $\delta = 2.099$ ppm (i.e., a shift of -0.013 ppm) upon diluting a sample from 4.6 mM to 0.31 mM. In comparison, Iyoda and co-workers[5] observed a significant upfield shift of -0.135 ppm for the TTF-CO_2CH_2 protons on **1c** when diluting a sample from 4.10 mM to 0.310 mM. The noticeable downfield shift experienced by **1c** at higher concentrations was interpreted as resulting from considerable aggregation in benzene. Thus substitution of the peripheral ester substituents (in **1c**) for hexyl groups (in **1d**) profoundly changes the propensity of the TTF–annulene to aggregate as judged from ^{1}H NMR data.

Absorption spectroscopy: UV/Vis absorption data for the two new compounds **1d** and **10** are collected in Table 1 together with literature data for **1b** and **1c**.[5] Compound **10** shows a longest wavelength absorption at $\lambda_{max} = 461$ nm (2.7 eV) in $CHCl_3$, while this band is significantly red-shifted for annulene **1d** ($\lambda_{max} = 532$ nm, 2.3 eV) (Figure 1). Moreover, **1d** exhibits a new broad absorption band/tail that extends to approximately 790 nm (1.6 eV). This broad band is ascribed to an intramolecular charge transfer from the peripheral TTF donors to the electron-accepting all-carbon core (vide infra).[7] The characteristic absorption maximum of **1d** at $\lambda_{max} = 532$ nm is red-shifted relative to **1b** and **1c** ($\lambda_{max} = 496$ nm for **1b**/**c** in CH_2Cl_2), but has a somewhat smaller molar absorptivity. Thus, the nature of the peripheral substitution has a substantial influence on the absorption characteristics. The absorption properties of **1d** were investigated in a selection of solvents (see Supporting Information), and a small degree of solvatochromism is observed in CS_2, in which the absorption maxima are red-shifted.

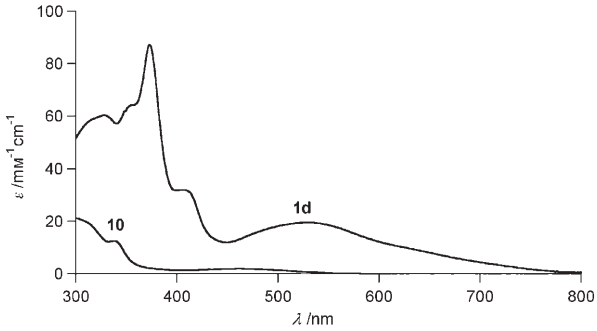

Figure 1. Electronic absorption spectra of **1d** and **10** in chloroform.

Importantly, we find that in both toluene and 2-methyltetrahydrofuran, the absorption spectrum of **1d** is concentration independent (in the concentration range from 7×10^{-6} M to 1.5×10^{-4} M) and follows the Lambert–Beer law, indicating that no aggregation of the macrocycle takes place. This observation is in agreement with the ^{1}H NMR spectroscopic study (vide supra). Not even upon cooling a sample (from 27 °C to −73 °C in toluene; from 27 °C to −173 °C in 2-methyltetrahydrofuran) were any indications of spectral shifts observed. In contrast, absorption spectroscopy supported strong aggregation of macrocycles **1b** and **1c** in toluene.[5]

Electrochemistry: Cyclic voltammetry data in CH_2Cl_2 (+0.1 M nBu$_4$NPF$_6$; all potentials referenced against the ferricinium/ferrocene couple (Fc^+/Fc)) are collected in Table 2. Compound **10** experiences two well-resolved reversible 1 e$^-$ oxidations at +0.00 and +0.52 V. For comparison, the parent tetrathiafulvalene (TTF) undergoes the two 1 e$^-$ oxidation steps at −0.08 and +0.40 V under the same conditions.[20] Thus, both oxidations of **10** are rendered more difficult by the introduc-

Table 1. UV/Vis absorption maxima (λ_{max} [nm]) and logarithmic molar extinction coefficients ($\log\varepsilon$) given in parentheses.[a]

	Solvent	λ_{max} [nm][b] ($\log\varepsilon$)						
1b[c]	CH_2Cl_2	308 [4.0] (4.83)	344 [3.6] (sh, 4.83)	359 [3.5] (4.89)	397 [3.1] (sh, 4.57)	496 [2.5] (4.46)	685 [1.8] (sh, 3.43)	
1c[c]	CH_2Cl_2	308 [4.0] (4.85)	344 [3.6] (sh, 4.85)	359 [3.5] (4.92)	397 [3.1] (sh, 4.56)	496 [2.5] (4.49)	685 [1.8] (sh, 3.37)	
1d	$CHCl_3$	314 [3.9] (sh, 4.77)	328 [3.8] (4.78)	355 [3.5] (sh, 4.81)	373 [3.3] (4.94)	407 [3.0] (sh, 4.51)	532 [2.3] (br, 4.29)	590–790 [1.6-2.1] (br t)
10	$CHCl_3$	263 [4.7] (sh, 4.19)	299 [4.1] (4.33)	338 [3.7] (sh, 4.10)	461 [2.7] (br, 3.26)			

[a] sh = shoulder; br = broad; t = tail. [b] The value in square brackets is the absorption maximum in eV. [c] Reference [5].

Table 2. Electrochemical data measured in CH_2Cl_2 + 0.1 M nBu_4NPF_6. All potentials versus Fc^+/Fc. Working electrode: glassy carbon electrode; counter electrode: Pt; reference electrode: Ag/AgCl. Scan rate: 0.1 Vs^{-1}.

Compound	E^{o}[a] [V]	ΔE_p[b] [mV]	E_p[c] [V]
1d	+0.20	90	
	+0.64	110	
			+1.20
			−1.40
			−1.70
10	+0.00	60	
	+0.52	65	
TTF	−0.08	60	
			+0.40[d]

[a] $E^{o}=(E_{pc}+E_{pa})/2$, in which E_{pc} and E_{pa} correspond to the cathodic and anodic peak potentials, respectively. [b] $\Delta E_p=E_{ox}-E_{red}$, in which subscripts ox and red refer to the conjugated oxidation and reduction steps, respectively. [c] Peak potential E_p for irreversible electron transfer. [d] Deposition on electrode surface.

tion of the two electron-withdrawing alkynyl residues. Macrocycle **1d** undergoes two reversible oxidation steps at +0.20 and +0.64 V as well as two irreversible reductions with peak potentials at −1.40 and −1.70 V. As shown in Figure 2, a third irreversible oxidation (E_{pa} = +1.20 V) is observed on the anodic electrolyte discharge. The peak amplitude for the first two oxidations is about three times larger than for the first reduction. It seems therefore reasonable to assume that the first oxidation involves three electrons and occurs on the three TTF moieties, generating the tris-radical cation $\mathbf{1d}^{3+}/(TTF^{\bullet+})_3$, whereas the second oxidation yields the hexacation $\mathbf{1d}^{6+}/(TTF^{2+})_3$. In contrast, the first reduction is a one-electron step occurring on the conjugated all-carbon macrocycle. In agreement with the strong electron-accepting nature of the inner core, the TTF moieties in **1d** are poorer electron donors than the TTF moiety in dialkynylated **10** (first oxidation at +0.00 V). Each TTF unit in **1d** can also be considered to be functionalized with two butadiynyl groups that are stronger electron acceptors than two ethynyl groups as present in **10**. The cyclic voltammogram reported by Iyoda and co-workers[5] for macrocycle **1b** showed oxidations to the tri- and hexacation at 0.43 V (broad) and 0.70 V, respectively, versus Fc^+/Fc in CH_2Cl_2. Thus, these potentials are significantly anodically shifted relative to those of **1d** on account of the electron-withdrawing ester groups.

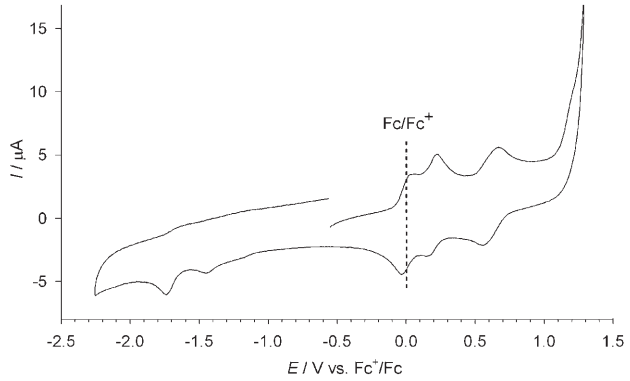

Figure 2. Cyclic voltammetry of **1d** in CH_2Cl_2 (+0.1 M nBu_4NPF_6) in the presence of ferrocene on a GC working electrode at a scan rate of 0.1 Vs^{-1}.

Analysis of the CV parameters as a function of scan rate revealed that adsorption occurs during the first oxidation of **1d**. Indeed the corresponding anodic peak current is proportional to the scan rate, characteristic of a weak adsorption of the reactant.[21] In contrast, the second oxidation behaves as a reversible electron transfer. The peak potential is scan rate independent; the peak current ratio is equal to unity, and a linear correlation between the peak current and the square root of the scan rate is observed. However, the peak potential difference is equal to 90 mV for the first oxidation and 110 mV for the second oxidation. These characteristics indicate that small interactions between the TTF redox centers occur, which is expected due to the macrocyclic conjugation. These interactions are larger for the second oxidation, since a peak potential difference of only 60 mV would have been expected for three independent redox centres.[22]

Spectroelectrochemical investigation of **10** gave a nice spectral evolution for both oxidation steps as shown in the Supporting Information. The initial spectrum was recovered quantitatively, which means that the generated species is stable. The generated radical cation $\mathbf{10}^{\bullet+}$ is characterized by absorptions at λ_{max} = 412, 468, and 713 nm (3.0, 2.6, and 1.7 eV), while the dication $\mathbf{10}^{2+}$ has a strong absorption at λ_{max} = 537 nm (2.3 eV). Several studies have been performed on TTF.[23] Thus, $TTF^{\bullet+}$ experiences absorption maxima at λ_{max} = 430 and 580 nm (2.9 and 2.1 eV) in MeCN and an absorption at λ_{max} = 714 nm (1.7 eV) in EtOH at 225 K that has been assigned to the π dimer TTF_2^{2+}. The ability of TTF radical cations to dimerize depends strongly on the substitution pattern and the absorption of $\mathbf{10}^{\bullet+}$ at 713 nm may be an intrinsic absorption of the radical cation rather than implying π-dimer formation.[23d] TTF^{2+} absorbs at λ_{max} = 390 nm (3.2 eV) in MeCN, that is, at significantly higher energy than the absorption of $\mathbf{10}^{2+}$.

Spectroelectrochemical studies on **1d** carried out during oxidation showed for the first oxidation step nice isosbestic points (electrolysis at +0.30 V versus Fc^+/Fc; Figure 3). The initial spectrum could be recovered quantitatively by reduction of the electrogenerated oxidized species at 0 V versus Fc^+/Fc. The evolving absorption bands at λ_{max} = 425, 467, and 705 nm (2.9, 2.7, and 1.8 eV) are attributed to the trication $\mathbf{1d}^{3+}$. For the second oxidation step (electrolysis at +0.80 V versus Fc^+/Fc; Figure 4), only one isosbestic point could be observed. A broad absorption around 530 nm (2.3 eV) evolves. Reduction of the generated species led only to the recovery of about 90% of the initial spectrum on account of some degradation of the generated species. As the absorption spectra of oxidized **1d** and **10** resemble each other, it seems reasonable to assume that the two oxidation steps of **1d** involve three electrons each. Still, howev-

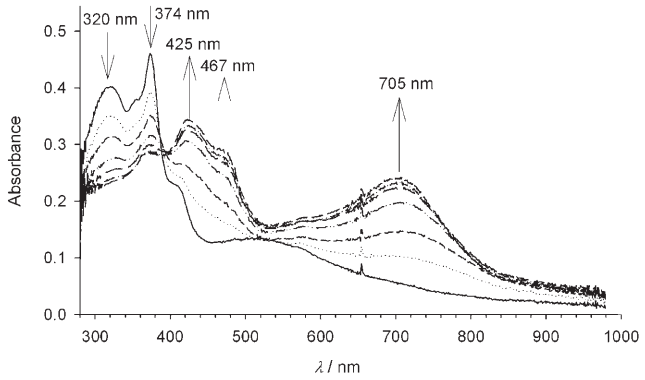

Figure 3. Time-resolved UV/Vis spectroelectrochemical investigation of **1d** in CH_2Cl_2 + 0.1 M nBu_4NPF_6 for the first oxidation step at +0.30 V versus Fc^+/Fc.

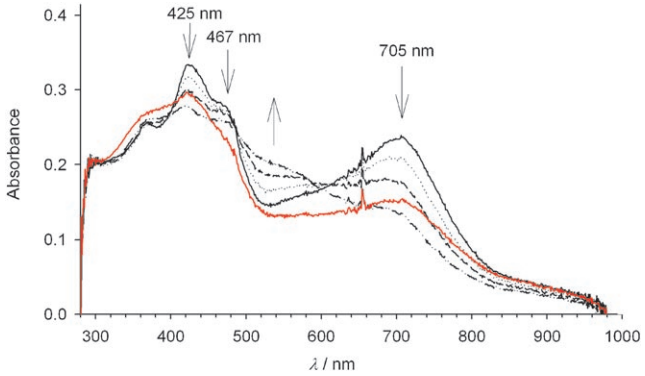

Figure 4. Time-resolved UV/Vis spectroelectrochemical investigation of **1d** in CH_2Cl_2 + 0.1 M nBu_4NPF_6 for the second oxidation step. The initial spectrum corresponds to the species obtained after the first oxidation step. The final spectrum after oxidation at +0.80 V and subsequent reduction at +0.30 V versus Fc^+/Fc is shown in red.

er, the three TTF units are not independent redox centers as judged from the peak potential difference.

Computational study: A computational study was performed on macrocycle **1a** and its monomeric precursor **2a**, both devoid of peripheral substituents, by employing the Gaussian 03 program package.[24] The molecules were geometry-optimized at the semiempirical PM3 level, and then single-point calculations were performed at the DFT level (B3LYP/6–311+G(2d,p)). The frontier orbitals resulting from these calculations are presented in Figures 5 and 6. It transpires that the HOMO and HOMO−1 (degenerate) of **1a** are mainly situated at the TTF units, while the LUMO and LUMO+1 (degenerate) are situated predominantly at the central core. Thus, the lowest energy absorption of **1a** has significant charge-transfer character. Single-point energies of the neutral and radical cations of **1a** and **2a** provide vertical ionization energies of 5.92 eV and 6.36 eV, respectively. Thus, as would be expected, the donor properties are enhanced in the gas phase for **1a** as compared to **2a**. For comparison, the first vertical ionization energy of the parent

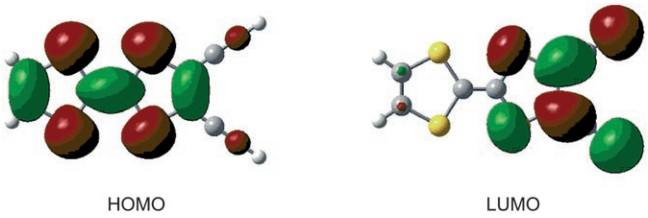

Figure 5. Frontier orbitals of **2a** (B3LYP/6–311+G(2d,p)).

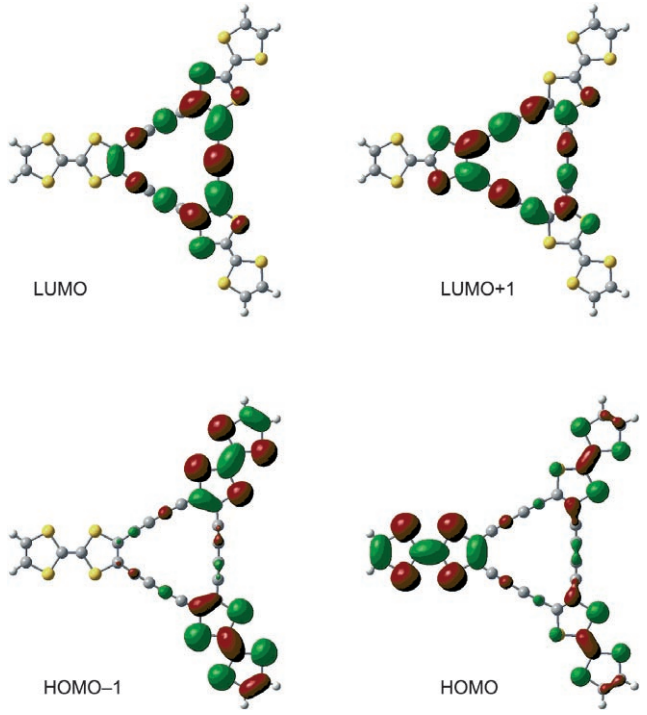

Figure 6. Frontier orbitals of **1a** (B3LYP/6–311+G(2d,p)). The HOMO−1 and HOMO are degenerate, as are the LUMO and LUMO+1.

TTF is 6.49 eV.[25] Thus, the donor strength decreases in the gas phase along the sequence **1d** > **10** > TTF, while it decreases along the opposite sequence TTF > **10** > **1d** in solution. That donor properties in solution and gas phase can be difficult to correlate was previously observed for alkyne-extended TTFs.[6f]

Surface study: Figure 7 shows the surface morphology of a drop-cast solution of **1d** in chloroform on a mica substrate. When the chloroform (approx 1 mg mL^{-1}) evaporates, it forms a particular structure at the edge of the drop-cast area, as seen in Figure 7A, which shows an optical differential interference contrast (DIC) image of the sample. The morphology of the edge of the drop-cast area is characterized by a thin band of crystalline domains as seen in the central part of Figure 7A. This observation suggests an ordered structure in which the molecules form crystalline domains with slightly different orientations. To verify this, the region displayed in Figure 7A was studied under an atomic force

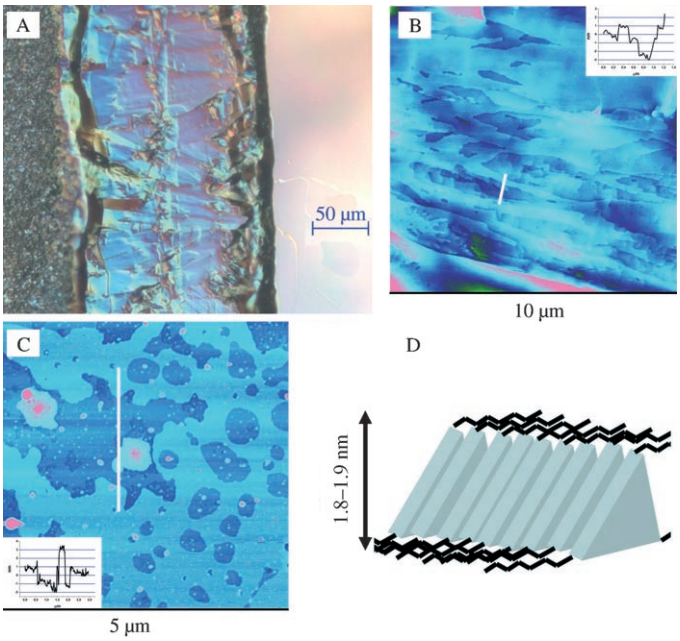

Figure 7. The structure of a drop-cast film from chloroform solution of **1d**. A) An optical differential interference coherence image of the edge of a drop-cast film. A thin band of crystalline domains is visible in the center of the image; the pink area to the right is the freshly cleaved mica surface on which the films were drop-cast. B) A representative 10 μm × 10 μm AFM recording of the surface of a crystalline domain located in the thin band seen in A). C) A representative 5 μm × 5 μm AFM recording of the surface of a very thin drop-cast film. The insets in both B and C are topography cross sections extracted at the white lines in the AFM recordings. The cross sections indicate that the thickness of the monolayer in both cases is just below 2 nm. D) A cartoon model of a possible arrangement of the molecules, giving rise to the layered structure seen in both B and C. The thickness of the molecules, standing edge on the surface with the side chains smeared out on the stacked molecules, is close to the observed value of 1.8–1.9 nm.

microscope (AFM). An example of how the surface appeared in the AFM in the thin band of domains is displayed in Figure 7B, which is a 10 × 10 μm AFM tapping mode recording. The molecules appear to form a layered structure with abrupt edges. The direction of the image is such that the right-hand side is toward the edge of the drop-cast area, indicating that the molecules are deposited in successive monolayers as the chloroform evaporates from the region, thus creating the distinct step-like morphology seen in the image. We also created a monolayer of the molecule by drop-casting a very dilute solution (less than 0.1 mg mL^{-1}) onto a mica substrate, but instead of waiting for the drop to dry, we sucked away the excess chloroform by touching the edge of the drop with a piece of filter paper. The chloroform in the thin meniscus of solution left behind evaporated shortly after, leaving behind an incomplete monolayer as seen in Figure 7C. The thicknesses of the monolayers seen in Figure 7B and 7C are almost identical: 1.9 nm (SD 0.2) for the layers seen in B and 1.8 nm (SD 0.1) for the layer seen in C. From the geometry optimization (vide supra) of **1a**, a diameter of the macrocycle (excluding the side chains) of 1.8–1.9 nm is estimated. We therefore assume that **1d** forms layered stacks as shown schematically in Figure 7D. The molecules are probably slightly titled and the hexyl chains smear out along the top and bottom plane of the layer. Interestingly, Iyoda and co-workers observed that **1b** formed threads on a silicon wafer that dried to a fibrous structure.[5]

Conclusion

Cyclization of the diethynylated TTF **10** after desilylation under Glaser–Hay oxidative conditions provides an efficient route to the well-soluble tris(tetrathiafulvaleno)dodecadehydro[18]annulene **1d** with six peripheral hexyl substituents. According to both ^{1}H NMR and UV/Vis absorption spectroscopy studies, the macrocycle shows basically no aggregation in solution. This behavior strongly contrasts that of TTF–annulenes containing peripheral carboxylic ester substituents.[5] The strong violet color of **1d** is accordingly assigned to an intramolecular charge-transfer transition rather than to an intermolecular one. The three TTF moieties in **1d** are oxidized in two three-electron steps. The number of electrons involved in each step is supported by spectroelectrochemical characterization of the oxidized species formed from **1d** and **10**. The first oxidation of **10** is cathodically shifted by +0.20 V relative to that of **1d**; that is, the TTF moieties of the macrocyclic system are more difficult to oxidize due to the strong electron-accepting properties of the all-carbon core. In contrast, we find that the calculated first vertical ionization energy of the parent compound **1a** (devoid of hexyl substituents) is 0.44 eV lower than that of **2a**. Drop-cast films of macrocycle **1d** show crystalline domains with slightly different orientations. AFM studies suggest that the molecules are deposited in successive monolayers as the chloroform evaporates from the region. Drop-casting of a very thin solution gave monolayers of thicknesses 1.8–1.9 nm, which correspond to the diameter of the macrocycle. Thus, the molecules seem to stack as schematically depicted in Figure 7D.

A very important lesson concerning the π-stacking aggregation tendency of dodecadehydro[18]annulenes is learned through comparison of the results presented in this paper for **1d** and those reported by Iyoda and co-workers for the ester-substituted derivatives **1b** and **1c**. In previous work on dodecadehydro[18]annulenes,[7,19b,26] perethynylated or fused with their olefinic moieties to other rings, we never had observed substantial aggregation tendencies. In other words, the Lambert–Beer law was obeyed and the ^{1}H NMR chemical shifts were nearly concentration-independent. The same behavior is observed for **1d**, and we conclude that the π-stacking aggregation tendency is negligible and not an intrinsic property of these acetylenic macrocycles, including the TTF derivatives. Therefore, we explain the very interesting self-assembly results reported by Iyoda and co-workers with the presence of the six ester groups. These groups render the entire π chromophore more electron-deficient, which favors π stacking.[10] They also extend the conjugated

π perimeter, but most importantly, they can undergo intermolecular dipolar interactions[8,9] that ultimately lead to the observed self-assembly. The fact that **1b** and **1c** only show aggregation in benzene or toluene, but not in the more polar solvents $CDCl_3$, CH_2Cl_2, or THF, further corroborates the role of dipolar interactions in the self-association process, since such interactions are highly dependent on the dielectric constant of the environment. We therefore feel that the entire body of studies reported here and elsewhere by Iyoda and co-workers[5] suggests that aromatic π-stacking self-assembly can be strongly enhanced by additional intermolecular dipolar interactions between appropriate functional groups.

Experimental Section

General methods: Chemicals were purchased from Acros, Fluka, or Aldrich and used as received. THF was distilled from sodium/benzophenone. Acetonitrile was dried over 4 Å molecular sieves. Technical grade solvents were distilled before use. Hay catalyst refers to a freshly prepared solution of CuCl (100 mg, 1.0 mmol) and *N,N,N′,N′*-tetramethylethylenediamine (TMEDA; 0.15 mL, 1.0 mmol) in CH_2Cl_2 (25 mL). Reactions were carried out under dry N_2 or Ar. TLC: pre-coated silica gel plates Alugram UV254 (Macherey-Nagel). Column chromatography: Kieselgel 60 (Fluka, particle size 0.040–0.063 mm). Deactivation of SiO_2 was done by flushing the column with 10% Et_3N in hexane and then washing with hexane. NMR: Varian Gemini 300 spectrometer; chemical shifts (δ) are given in ppm relative to TMS; coupling constants (J) are given in Hz; solvent signals were used as internal references. Infrared spectra (IR) were recorded on a Varian 800 FT-IR spectrometer. EI-MS spectra were measured on a Hitachi–Perkin–Elmer VG-TRIBID spectrometer; ESI-MS spectra were measured on a Finnigan Mat TSQ 7000 spectrometer. High resolution (HR) FT-MALDI spectra were measured on an Ionspec Ultima Fourier transform instrument with 3-hydroxypicolinic acid (3-HPA) in MeOH/H_2O as matrix, and the compound in CH_2Cl_2 (two-layer technique). Differential scanning calorimetry (DSC) was carried out on a Mettler Toledo DSC 822 under nitrogen flow, at a heating rate of 2 °C min^{-1} between 25 °C and 250 °C. Melting points were measured on a Büchi B-540 melting-point apparatus in open capillaries and are uncorrected. Elemental analyses were performed by the Mikrolabor at the Laboratorium für Organische Chemie, ETH Zürich.

Electrochemistry: Electrochemical measurements were carried out in CH_2Cl_2 containing 0.1 M nBu$_4$NPF$_6$ in a classical three-electrode cell by cyclic voltammetry (CV) and rotating-disk voltammetry (RDV). The working electrode was a glassy carbon (GC) disk (2 mm in diameter), the auxiliary electrode a Pt wire, and the reference electrode an aqueous Ag/AgCl electrode. The cell was connected to an Autolab PGSTAT20 potentiostat (Eco Chemie, Holland) driven by a GPSE software running on a personal computer. All potentials are given versus Fc^+/Fc used as internal reference and are uncorrected from ohmic drop. Spectroelectrochemical studies were also carried out in the same medium, in a home-made OTTLE cell[27] placed in a diode array spectrophotometer HP 8453.

UV/Vis spectroscopy: UV/Vis spectra were recorded on a Varian Cary 500 or a Varian Cary 50 spectrophotometer, using the pure solvent as baseline. Low-temperature spectra were recorded using a temperature controlled liquid nitrogen Oxford cryostat (OptistatDN).

Drop-cast and AFM: The drop-cast films were made from a solution of 1 mg mL^{-1} of **1d** in HPLC-grade chloroform. The monolayer was created using a very thin (< 0.1 mg mL^{-1}) solution of **1d** in HPLC-grade chloroform. The films were drop-cast on a freshly cleaved mica surface and were allowed to dry under ambient conditions. The AFM images were recorded with a Nanoscope IIIa from Veeco Instruments, working in tapping mode, by using a silicon tapping mode tip from Olympus (300 kHz), under ambient conditions (23 °C). The optical image in Figure 7A was obtained by a Zeiss axiotech setup for differential interference contrast with 20×10 magnification.

8-Chlorotetradecan-7-one (4): PPh_3 (7.38 g, 28.1 mmol) was added to a solution of **3** (4.94 g, 21.6 mmol) in MeCN (100 mL). The mixture was cooled to 10 °C, and CCl_4 (10.5 mL, 108 mmol) was added by syringe. After the addition, the mixture was allowed to reach 20 °C and was stirred for 1 h. MeOH (30 mL) was added and the solution stirred for 0.5 h and concentrated in vacuo. The residue was dissolved in a minimum of CH_2Cl_2 and passed through a short silica column (hexane/EtOAc 9:1) to afford **4** as a colorless oil (5.19 g, 97%). ^{1}H NMR (300 MHz, $CDCl_3$): δ = 4.19 (dd, ^3J = 5.6 Hz, ^3J = 8.4 Hz, 1H), 2.64 (t, ^3J = 6.9 Hz, 2H), 2.0–1.2 (m, 18H), 0.88 ppm (t, ^3J = 6.9 Hz, 6H); ^{13}C NMR (75 MHz, $CDCl_3$): δ = 205.5, 63.8, 38.6, 33.9, 31.6, 31.5, 28.8, 28.7, 26.1, 23.7, 22.6 (×2), 14.1 ppm (×2); IR (neat): $\tilde{\nu}$ = 2956 (m), 2927 (s), 2858 (s), 1719 (s), 1462 (s), 1406 (w), 1377 (m), 725 (m), 630 cm^{-1} (s); EI-MS (70 eV): m/z (%): 246 (0.5) $[M]^+$, 113 (100) $[C_7H_{13}O]^+$; HR-EI-MS: m/z calcd for $C_{14}H_{27}ClO$: 246.1745; found: 246.1742; elemental analysis (%) calcd for $C_{14}H_{27}ClO$ (246.82): C 68.13, H 11.03; found: C 68.13, H 11.12.

1-Hexyl-2-oxooctyl piperidine-1-carbodithioate (5): Potassium piperidine-1-carbodithioate (4.40 g, 22.0 mmol) was added to a solution of **4** (5.19 g, 21.0 mmol) in acetone (100 mL), and the mixture stirred at 20 °C for 3 h. The solvent was removed in vacuo, and Et_2O (200 mL) was added. The resulting mixture was extracted with H_2O (3×100 mL), the water phase extracted with Et_2O (100 mL), and the combined organic phases dried ($MgSO_4$), filtered, and concentrated in vacuo. Column chromatography (SiO_2, hexane/EtOAc 93:7) gave **5** (6.86 g, 88%) as a colorless oil. ^{1}H NMR (300 MHz, $CDCl_3$): δ = 4.95 (t, ^3J = 7.2 Hz, 1H), 4.25 (br s, 2H), 3.91 (br s, 2H), 2.8–2.5 (m, 2H), 2.0–1.5 (m, 8H), 1.4–1.2 (m, 16H), 0.86 ppm (t, ^3J = 6.9 Hz, 6H); ^{13}C NMR (75 MHz, $CDCl_3$): δ = 207.9, 193.8, 59.8, 53.5, 51.6, 41.6, 31.7, 31.6, 30.4, 29.1, 28.8, 27.3, 26.1, 25.5, 24.3, 23.8, 22.6 (×2), 14.1 ppm (×2); IR (neat): $\tilde{\nu}$ = 2926 (s), 2856 (s), 2360 (w), 1711 (s), 1475 (m), 1427 (s), 1361 (w), 1280 (w), 1242 (s), 1227 (s), 1134 (w), 1113 (w), 1005 (w), 974 (w), 891 (w), 853 cm^{-1} (w); EI-MS (70 eV): m/z (%): 371 (0.8) $[M]^+$, 211 (48) $[C_{14}H_{27}O]^+$, 128 (100) $[C_6H_{10}NS]^+$; HR-EI-MS calcd for $C_{20}H_{37}NOS_2$: 371.2312; found: 371.2313; elemental analysis (%) calcd for $C_{20}H_{37}NOS_2$ (371.64): C 64.64, H 10.03, N 3.77, S 17.26; found: C 64.77, H 10.03, N 3.90, S 17.14.

***N*-(4,5-Dihexyl-1,3-dithiol-2-ylidene)piperidinium hexafluorophosphate (6)**: Compound **5** (6.86 g, 18.5 mmol) was added dropwise to a stirred ice-cold solution of concentrated sulfuric acid (15 mL). After the addition, the mixture was allowed to reach 20 °C, stirred for 4 h, and then poured slowly into H_2O (65 mL) containing HPF_6 (2.35 mL, 65 wt% in H_2O, 18.5 mmol) and cooled to 0 °C. CH_2Cl_2 (150 mL) was added and the phases separated. The water phase was extracted with CH_2Cl_2 (2× 50 mL), and the combined organic phases were washed sequentially with water (50 mL), saturated aqueous $NaHCO_3$ (50 mL), and water (50 mL), dried ($MgSO_4$), filtered, and concentrated in vacuo to yield **6** (7.85 g, 85%) as a viscous orange oil of sufficient purity for further reaction. An analytically pure sample was obtained by column chromatography (SiO_2, hexane/acetone 3:2). ^{1}H NMR (300 MHz, $CDCl_3$): δ = 3.81 (t, ^3J = 6.5 Hz, 4H), 2.64 (t, ^3J = 7.8 Hz, 4H), 1.95–1.73 (m, 6H), 1.61 (m, 4H), 1.41–1.23 (m, 12H), 0.89 ppm (t, ^3J = 6.9 Hz, 6H); ^{13}C NMR (75 MHz, $CDCl_3$): δ = 184.4, 133.7, 56.6, 31.3, 30.3, 28.7, 28.6, 25.0, 22.5, 21.5, 14.1 ppm; IR (neat): $\tilde{\nu}$ = 2955 (w), 2930 (m), 2858 (w), 1609 (w), 1542 (m), 1448 (m), 1378 (w), 1258 (m), 1238 (w), 1115 (w), 1007 (w), 831 cm^{-1} (s); ESI-MS: m/z (%): 354 (100) $[C_{20}H_{36}NS_2]^+$; elemental analysis (%) calcd for $C_{20}H_{36}F_6NPS_2$ (499.60): C 48.08, H 7.26, N 2.80, S 12.84; found: C 47.99, H 7.49, N 2.79, S 13.04.

4,5-Dihexyltetrathiafulvalene (8): Trimethylphosphite (0.95 mL, 8.1 mmol) was added dropwise to a suspension of 1,3-dithiolium iodide[28] (1.71 g, 7.43 mmol) in dry MeCN (40 mL) cooled to 0 °C. After the addition was complete, the reaction was stirred at 20 °C for 0.5 h and concentrated in vacuo to give the crude phosphonate ester **7**,[15] which was dissolved in dry THF (40 mL) and cooled to −78 °C. BuLi (4.8 mL, 1.6 M in hexane, 7.7 mmol) was added dropwise and the milky white mixture stirred for 10 min, whereupon the crude hexafluorophosphate salt **6** (5.07 g, 10.2 mmol) in dry THF (5 mL) was added in one portion. The mixture was stirred for 15 min at low temperature and then heated to 20 °C and

stirred for another 45 min. Acetic acid (4.0 mL, 70 mmol) was added, the mixture stirred for 2 h, and the dark green solution concentrated in vacuo to a volume of about 10 mL. Et_2O (150 mL) was added and the mixture washed sequentially with H_2O (100 mL), saturated aqueous $NaHCO_3$ (100 mL), and H_2O (100 mL), and was then dried ($MgSO_4$), filtered, and concentrated in vacuo. Column chromatography (SiO_2, hexane/EtOAc 94:6) afforded **8** (2.02 g, 73%) as an orange oil. ^{1}H NMR (300 MHz, $CDCl_3$): $\delta = 6.28$ (s, 2H), 2.33 (t, $^3J = 7.3$ Hz, 4H), 1.50 (q, $^3J = 7.7$ Hz, 4H), 1.36–1.24 (m, 12H), 0.89 ppm (t, $^3J = 6.8$ Hz, 6H); ^{13}C NMR (75 MHz, $CDCl_3$): $\delta = 128.8$, 119.1, 109.2, 108.3, 31.5, 29.6, 28.8 (x 2), 22.5, 14.1 ppm; IR (neat): $\tilde{\nu} = 3069$ (w), 2953 (m), 2924 (s) , 2855 (s), 1464 (m), 1377 cm^{-1} (w); UV/Vis ($CHCl_3$): λ_{max} (ε) = 324 nm (11800); HR-EI-MS (70 eV) calcd for $C_{18}H_{28}S_4$ $[M]^+$: 372.1069; found: 372.1068; elemental analysis (%) calcd for $C_{18}H_{28}S_4$ (372.67): C 58.01, H 7.57, S 34.42; found: C 57.95, H 7.68, S 34.43.

4,5-Dihexyl-4′,5′-diiodotetrathiafulvalene (9): A freshly prepared solution of LDA (9.16 mL, 0.59 M in THF, 5.4 mmol) was added dropwise to a solution of **8** (0.960 g, 2.58 mmol) in THF (50 mL) cooled to −78 °C and the reaction mixture stirred at this temperature for 2 h. 1,2-Diiodoethane (1.52 g, 5.40 mmol) was added in one portion. The mixture was stirred for 1 h at −78 °C, then heated to 20 °C, and stirred for another 0.5 h. The red solution was partitioned between saturated aqueous $Na_2S_2O_3$ (150 mL) and Et_2O (150 mL), extracted with Et_2O (2 × 100 mL), and the combined organic phases were washed with water (100 mL), dried ($MgSO_4$), filtered, and concentrated in vacuo. Column chromatography (deactivated SiO_2, hexane/EtOAc 99:1) afforded **9** (1.42 g, 88%) as a red oil which solidified upon cooling. M.p. 46–47 °C; ^{1}H NMR (300 MHz, $CDCl_3$): $\delta = 2.32$ (t, $^3J = 7.5$ Hz, 4H), 1.48 (q, $^3J = 7.4$ Hz, 4H), 1.35–1.23 (m, 12H), 0.88 ppm (t, $^3J = 7.0$ Hz, 6H); ^{13}C NMR (75 MHz, $CDCl_3$): $\delta =$ 128.7, 124.3, 115.1, 110.8, 31.5, 29.7, 28.7 (×2), 22.5, 14.1 ppm; IR (neat): $\tilde{\nu} = 2949$ (s), 2920 (s), 2848 (s), 1612 (w), 1541 (w), 1466 (s), 1451 (m), 1375 (m), 1350 (w), 1316 (w), 1161 (w), 1113 (w), 914 (w), 895 (w), 831 cm^{-1} (m); UV/Vis ($CHCl_3$): λ_{max} (ε) = 292 (13000), 328 nm (13400); HR-EI-MS (70 eV) calcd for $C_{18}H_{26}I_2S_4$ $[M]^+$: 623.9002; found: 623.9000; elemental analysis (%) calcd for $C_{18}H_{26}I_2S_4$ (624.5): C 34.62, H 4.20, S 20.54; found: C 34.87, H 4.11, S 20.63.

4,5-Bis(triisopropylsilylethynyl)-4′,5′-dihexyltetrathiafulvalene (10): [Pd-$(PPh_3)_2Cl_2$] (130 mg, 0.185 mmol) and CuI (70 mg, 0.37 mmol) were added to a degassed solution of **9** (1.19 g, 1.91 mmol) and triisopropylsilylacetylene (1.03 mL, 4.58 mmol) in Et_3N (50 mL). The mixture was stirred at 20 °C under N_2 for 24 h, filtered through a plug of silica gel (hexane), and concentrated in vacuo. Column chromatography (SiO_2, hexane) gave **10** (959 mg, 69%) as a dark red oil. ^{1}H NMR (300 MHz, $CDCl_3$): $\delta = 2.33$ (t, $^3J = 7.5$ Hz, 4H), 1.49 (q, $^3J = 7.5$ Hz, 4H), 1.36–1.24 (m, 12H), 1.08 (s, 42H), 0.89 ppm (t, $^3J = 6.9$ Hz, 6H); ^{13}C NMR (75 MHz, $CDCl_3$): $\delta = 128.6$, 121.3, 114.7, 103.6, 102.5, 96.6, 31.5, 29.7, 28.8 (×2), 22.5, 18.6, 14.1, 11.1 ppm; IR (neat): $\tilde{\nu} = 2941$ (m), 2926 (s), 2864 (s), 2359 (w), 2342 (w), 2141 (w), 1676 (w), 1462 (s), 1383 (w), 1368 (w), 1244 (w), 1211 (w), 1069 (s), 1019 (w), 996 (m), 920 (w), 882 cm^{-1} (s); UV/Vis ($CHCl_3$): λ_{max} (ε) = 299 (21200), 338 (sh, 12500), 461 nm (1800); HR-FT-MALDI-MS (3-HPA): *m/z* calcd for $C_{40}H_{68}S_4Si_2$ $[M]^+$: 732.3737; found: 732.3724; elemental analysis (%) calcd for $C_{40}H_{68}S_4Si_2$ (733.4): C 65.51, H 9.34, S 17.49; found: C 65.57, H 9.43, S 17.21.

Hexahexyl-1,2,7,8,13,14-tris(tetrathiafulvaleno)-3,4,5,6,9,10,11,12,15,16,17,18-dodecahydro[18]annulene (1d): nBu$_4$NF (0.65 mL, 1 M in wet THF, 0.65 mmol) was added to a solution of **10** (223 mg, 0.304 mmol) in THF (15 mL) cooled to 0 °C, and the dark red solution stirred for 10 min. CH_2Cl_2 (10 mL) was added, and the mixture filtered through a plug of silica gel (hexane/CH_2Cl_2 1:1). Most of the solvent was removed under reduced pressure to give **11** as a dark red oil, which was dissolved in CH_2Cl_2 (30 mL) and cooled to 0 °C. Hay catalyst (6 mL) was added and the mixture stirred at this temperature open to air for 1 h. Et_3N (2 mL) was added and the mixture filtered through a plug of silica gel (hexane/CH_2Cl_2 1:1) and concentrated in vacuo. Column chromatography (SiO_2, hexane/CH_2Cl_2 1:2) afforded **1d** (60 mg, 47%) as a dark purple, metallic solid. M.p. (DSC) ~100 °C (decomp); ^{1}H NMR (300 MHz, $CDCl_3$): $\delta = 2.38$ (t, $^3J = 7.5$ Hz, 12H), 1.52 (m, 12H), 1.31 (m, 36H), 0.90 ppm (t, $^3J = 6.7$ Hz, 18H); ^{13}C NMR (75 MHz, $CDCl_3$): $\delta =$ 128.7, 125.2, 85.1, 79.6, 31.5, 29.8, 28.8 (2C), 22.5, 14.1 ppm; IR (neat): $\tilde{\nu} = 2953$ (m), 2920 (s), 2851 (s), 2172 (w), 2124 (w), 1611 (w), 1458 (s), 1377 (s), 1096 (s), 1046 (w), 1012 (w), 937 (m), 924 (m), 909 (m), 777 (s), 722 cm^{-1} (m); UV/Vis ($CHCl_3$): λ_{max} (ε) = 314 (sh, 58300), 328 (60400), 355 (sh, 64300), 373 (87000), 407 (sh, 32000), 532 (19500), 590–790 nm (br); HR-FT-MALDI-MS (3-HPA): *m/z* calcd for $C_{66}H_{78}S_{12}$ $[M]^+$: 1254.2747; found: 1254.2771; elemental analysis (%) calcd for $C_{66}H_{78}S_{12}$ (1256.11): C 63.11, H 6.26, S 30.63; found: C 63.37, H 6.14, S 30.41.

Acknowledgements

Financial support from the ETH Research Foundation and the Danish Research Agency (grant #2111-04-0018) is gratefully acknowledged. A.S.A. thanks the University of Copenhagen for a Ph.D. scholarship.

[1] a) M. R. Bryce, *Adv. Mater.* **1999**, *11*, 11–23; b) M. B. Nielsen, C. Lomholt, J. Becher, *Chem. Soc. Rev.* **2000**, *29*, 153–164; c) M. R. Bryce, *J. Mater. Chem.* **2000**, *10*, 589–598; d) J. L. Segura, N. Martín, *Angew. Chem.* **2001**, *113*, 1416–1455; *Angew. Chem. Int. Ed.* **2001**, *40*, 1372–1409; e) Special issue on molecular conductors (Ed.: P. Batail): *Chem. Rev.* **2004**, *104*, 4887–5781.

[2] a) F. Diederich, *Chem. Commun.* **2001**, 219–227; b) M. B. Nielsen, F. Diederich, *Synlett* **2002**, 544–552; c) M. B. Nielsen, F. Diederich, *Chem. Rec.* **2002**, *2*, 189–198.

[3] a) T. Yamamoto, T. Shimizu, *J. Mater. Chem.* **1997**, *7*, 1967–1968; b) S. Shimada, A. Masaki, K. Hayamizu, H. Matsuda, S. Okada, H. Nakanishi, *Chem. Commun.* **1997**, 1421–1422; c) T. Shimizu, T. Yamamoto, *Chem. Commun.* **1999**, 515–516; d) M. Iyoda, M. Hasegawa, J. Takano, K. Hara, Y. Kuwatani, *Chem. Lett.* **2002**, 590–591; e) K. Hara, M. Hasegawa, Y. Kuwatani, H. Enozawa, M. Iyoda, *Chem. Commun.* **2004**, 2042–2043; f) M. Hasegawa, J. Takano, H. Enozawa, Y. Kuwatani, M. Iyoda, *Tetrahedron Lett.* **2004**, *45*, 4109–4112; g) M. Iyoda, H. Enozawa, Y. Miyake, *Chem. Lett.* **2004**, *33*, 1098–1099; h) M. Iyoda, M. Hasegawa, Y. Miyake, *Chem. Rev.* **2004**, *104*, 5085–5113.

[4] D. Solooki, T. C. Parker, S. I. Khan, Y. Rubin, *Tetrahedron Lett.* **1998**, *39*, 1327–1330.

[5] H. Enozawa, M. Hasegawa, D. Takamatsu, K. Fukui, M. Iyoda, *Org. Lett.* **2006**, *8*, 1917–1920.

[6] a) M. B. Nielsen, N. N. P. Moonen, C. Boudon, J.-P. Gisselbrecht, P. Seiler, M. Gross, F. Diederich, *Chem. Commun.* **2001**, 1848–1849; b) M. B. Nielsen, N. F. Utesch, N. N. P. Moonen, C. Boudon, J.-P. Gisselbrecht, S. Concilio, S. P. Piotto, P. Seiler, P. Günter, M. Gross, F. Diederich, *Chem. Eur. J.* **2002**, *8*, 3601–3613; c) M. B. Nielsen, *Synlett* **2003**, 1423–1426; d) M. B. Nielsen, J.-P. Gisselbrecht, N. Thorup, S. P. Piotto, C. Boudon, M. Gross, *Tetrahedron Lett.* **2003**, *44*, 6721–6723; e) T. Kumagai, M. Tomura, J. Nishida, Y. Yamashita, *Tetrahedron Lett.* **2003**, *44*, 6845–6848; f) K. Qvortrup, M. T. Jakobsen, J.-P. Gisselbrecht, C. Boudon, F. Jensen, S. B. Nielsen, M. B. Nielsen, *J. Mater. Chem.* **2004**, *14*, 1768–1773; g) K. Qvortrup, A. S. Andersson, J.-P. Mayer, A. S. Jepsen, M. B. Nielsen, *Synlett* **2004**, 2818–2820; h) A. Gorgues, P. Hudhomme, M. Sallé, *Chem. Rev.* **2004**, *104*, 5151–5184; i) M. B. Nielsen, J. C. Petersen, N. Thorup, A. S. Jepsen, J.-P. Gisselbrecht, C. Boudon, M. Gross, *J. Mater. Chem.* **2005**, *15*, 2599–2605; j) A. S. Andersson, K. Qvortrup, E. R. Torbensen, J.-P. Mayer, J.-P. Gisselbrecht, C. Boudon, M. Gross, A. Kadziola, K. Kilså, M. B. Nielsen, *Eur. J. Org. Chem.* **2005**, 3660–3671; k) M. B. Nielsen, *Lett. Org. Chem.* **2006**, *3*, 3–9; l) Y.-L. Zhao, W. Zhang, J.-Q. Zhang, Q. Liu, *Tetrahedron Lett.* **2006**, *47*, 3157–3159.

[7] F. Mitzel, C. Boudon, J, -P. Gisselbrecht, P. Seiler, M. Gross, F. Diederich, *Helv. Chim. Acta* **2004**, *87*, 1130–1157.

[8] a) C. Grave, A. D. Schlüter, *Eur. J. Org. Chem.* **2002**, 3075–3098; b) Y. Tobe, N. Utsumi, K. Kawabata, A. Nagano, K. Adachi, S. Araki, M. Sonoda, K. Hirose, K. Naemura, *J. Am. Chem. Soc.* **2002**, *124*, 5350–5364; c) C.-H. Lin, J. Tour, *J. Org. Chem.* **2002**, *67*, 7761–

7768; d) D. Zhao, J. S. Moore, *Chem. Commun.* **2003**, 807–818; e) H. Li, E. A. Homan, A. J. Lampkins, I. Ghiviriga, R. K. Castellano, *Org. Lett.* **2005**, *7*, 443–446; f) C. S. Jones, M. J. O'Connor, M. M. Haley in *Acetylene Chemistry* (Eds.: F. Diederich, P. J. Stang, R. R. Tykwinski), Wiley-VCH, Weinheim, **2005**, pp. 303–385.

[9] R. Paulini, K. Müller, F. Diederich, *Angew. Chem.* **2005**, *117*, 1820–1839; *Angew. Chem. Int. Ed.* **2005**, *44*, 1788–1805.

[10] C. A. Hunter, J. K. M. Sanders, *J. Am. Chem. Soc.* **1990**, *112*, 5525–5534.

[11] J. M. Fabre, *Chem. Rev.* **2004**, *104*, 5133–5150.

[12] A. Miyashita, Y. Suzuki, K. Iwamoto, T. Higashino, *Chem. Pharm. Bull.* **1994**, *42*, 2633–2635.

[13] N. Karali, I. Apak, S. Özkirimli, A. Gürsoy, S. U. Dogan, A. Eraslan, O. Özdemir, *Arch. Pharm.* **1999**, *332*, 422–426.

[14] H. Mora, J.-M. Fabre, L. Giral, C. Montginoul, *Bull. Soc. Chim. Belg.* **1992**, *101*, 137–146.

[15] a) A. J. Moore, M. R. Bryce, *J. Chem. Soc. Perkin Trans. 1* **1991**, 157–168; b) M. Formigué, I. Johannsen, K. Boubekeur, C. Nelson, P. Batail, *J. Am. Chem. Soc.* **1993**, *115*, 3752–3759.

[16] K. Sonogashira in *Metal-Catalyzed Cross-Coupling Reactions* (Eds.: F. Diederich, P. J. Stang), Wiley-VCH, Weinheim, **1998**, pp. 203–229.

[17] a) P. Nguyen, Z. Yuan, L. Agocs, G. Lesley, T. B. Marder, *Inorg. Chim. Acta* **1994**, *220*, 289–296; b) E. V. Tretyakov, D. W. Knight, S. F. Vasilevsky, *J. Chem. Soc. Perkin Trans. 1* **1999**, 3713–3720; c) M.-Y. Chou, A. B. Mandal, M. Leung, *J. Org. Chem.* **2002**, *67*, 1501–1505; d) J. Zeidler, *Collect. Czech. Chem. Commun.* **2004**, *69*, 1610–1630.

[18] A. S. Hay, *J. Org. Chem.* **1962**, *27*, 3320–3321.

[19] a) J. Anthony, C. B. Knobler, F. Diederich, *Angew. Chem.* **1993**, *105*, 437–440; *Angew. Chem. Int. Ed. Engl.* **1993**, *32*, 406–409; b) J. Anthony, A. M. Boldi, C. Boudon, J.-P. Gisselbrecht, M. Gross, P. Seiler, C. B. Knobler, F. Diederich, *Helv. Chim. Acta* **1995**, *78*, 797–817.

[20] The redox potentials obtained for TTF are in accordance with literature values after calibrating those to the Fc^+/Fc redox couple: W. Devonport, M. R. Bryce, G. J. Marshallsay, A. J. Moore, L. M. Goldenberg, *J. Mater. Chem.* **1998**, *8*, 1361–1372.

[21] *Electrochemical Methods: Fundamentals and Applications*, 2nd ed. (Eds.: A. J. Bard, L. R. Faulkner), Wiley, **2001**, pp. 594–601.

[22] J. B. Flanagan, S. Margel, A. J. Bard, F. C. Anson, *J. Am. Chem. Soc.* **1978**, *100*, 4248–4253.

[23] a) J. B. Torrance, B. A. Scott, B. Welber, F. B. Kaufman, P. E. Seiden, *Phys. Rev. B* **1979**, *19*, 730–741; b) L. Huchet, S. Akoudad, E. Levillain, J. Roncali, A. Emge, P. Bäuerle, *J. Phys. Chem. B* **1998**, *102*, 7776–7781; c) H. Spanggaard, J. Prehn, M. B. Nielsen, E. Levillain, M. Allain, J. Becher, *J. Am. Chem. Soc.* **2000**, *122*, 9486–9494; d) V. Khodorkovsky, L. Shapiro, P. Krief, A. Shames, G. Mabon, A. Gorgues, M. Giffard, *Chem. Commun.* **2001**, 2736–2737.

[24] Gaussian 03, Revision B.03, M. J. Frisch, G. W. Trucks, H. B. Schlegel, G. E. Scuseria, M. A. Robb, J. R. Cheeseman, J. A. Montgomery, Jr., T. Vreven, K. N. Kudin, J. C. Burant, J. M. Millam, S. S. Iyengar, J. Tomasi, V. Barone, B. Mennucci, M. Cossi, G. Scalmani, N. Rega, G. A. Petersson, H. Nakatsuji, M. Hada, M. Ehara, K. Toyota, R. Fukuda, J. Hasegawa, M. Ishida, T. Nakajima, Y. Honda, O. Kitao, H. Nakai, M. Klene, X. Li, J. E. Knox, H. P. Hratchian, J. B. Cross, C. Adamo, J. Jaramillo, R. Gomperts, R. E. Stratmann, O. Yazyev, A. J. Austin, R. Cammi, C. Pomelli, J. W. Ochterski, P. Y. Ayala, K. Morokuma, G. A. Voth, P. Salvador, J. J. Dannenberg, V. G. Zakrzewski, S. Dapprich, A. D. Daniels, M. C. Strain, O. Farkas, D. K. Malick, A. D. Rabuck, K. Raghavachari, J. B. Foresman, J. V. Ortiz, Q. Cui, A. G. Baboul, S. Clifford, J. Cioslowski, B. B. Stefanov, G. Liu, A. Liashenko, P. Piskorz, I. Komaromi, R. L. Martin, D. J. Fox, T. Keith, M. A. Al-Laham, C. Y. Peng, A. Nanayakkara, M. Challacombe, P. M. W. Gill, B. Johnson, W. Chen, M. W. Wong, C. Gonzalez, J. A. Pople, Gaussian, Inc., Pittsburgh PA, **2003**.

[25] S. B. Nielsen, M. B. Nielsen, H. J. Aa. Jensen, *Phys. Chem. Chem. Phys.* **2003**, *5*, 1376–1380.

[26] a) Y. Rubin, C. B. Knobler, F. Diederich, *J. Am. Chem. Soc.* **1990**, *112*, 1607–1617; b) Y. Rubin, M. Kahr, C. B. Knobler, F. Diederich, C. L. Wilkins, *J. Am. Chem. Soc.* **1991**, *113*, 495–500; c) M. Kivala, F. Mitzel, C. Boudon, J.-P. Gisselbrecht, P. Seiler, M. Gross, F. Diederich, *Chem. Asian J.* **2006**, *1*, 479–489.

[27] C. Bernard, J.-P. Gisselbrecht, M. Gross, E. Vogel, M. Lausmann, *Inorg. Chem.* **1994**, *33*, 2393–2401.

[28] A. Moore, M. Bryce, *Synthesis* **1997**, 407–409.

Received: July 10, 2006
Published online: October 11, 2006

